

OPTIMIZATION OF THE VERTICAL COMFORT AND SAFETY OF A GROUND VEHICLE

Walter Jesus Paucar Casas, walter.paucar.casas@ufrgs.br

Maurício Mazzutti, mauricio.mazzutti@ufrgs.br

Venâncio Lázaro Batalhone Neto, batalhone-2@bol.com.br

Universidade Federal do Rio Grande do Sul, Departamento de Engenharia Mecânica, Rua Sarmento Leite 425, CEP 90050-170, Porto Alegre – RS, Brazil

Abstract. A nonlinear optimization methodology is applied to improve the vertical dynamics involving comfort and safety of ground vehicles implemented with passive suspensions. The methodology takes advantage of the *fmincon* algorithm of MATLAB® to find the minimum of a constrained nonlinear multivariable function and the vehicle model is developed through the dynamics of multibody systems. The design variables include suspension parameters such as the stiffness and the damping coefficients. Some inputs are considered fixed throughout the optimization, such as the random profile of a secondary road of very low quality. The obtained results show that the nonlinear optimization algorithm is an adequate tool for improving the vertical comfort and safety of ground vehicles.

Keywords: vehicle dynamics, vertical comfort and safety, nonlinear optimization, passive suspension.

1. INTRODUCTION

The behavior of the vertical dynamics of a vehicle results from a variety of interaction variables: the conductor, the type of vehicle, the involved loads and the road where the vehicle transits. The optimization of the vertical dynamics of a vehicle is directly involved with the improvement of the comfort and the safety, and indirectly with the reduction of the damage to the road.

The determinations of the parameters that influence the dynamics of the vehicle are based on results of laboratory, field tests and still in computational simulations. This work looks for the optimal vertical dynamic behavior, where the variables of the problem are the coefficients of damping and stiffness of the suspensions. For doing that, a complete vehicle is modeled and submitted to a random excitation of the road. To describe the dynamics of the vehicle, one model with seven degrees of freedom is considered, where the suspensions are independent between them.

2. VEHICLE MODEL

For the mathematical analysis of the problem, a complete model of the vehicle with seven degrees of freedom is adopted, based on the proposal of Ikenaga *et al.* (2000) and used by Motta and Zampieri (2005). The model consists in a sprung mass (body of the vehicle) linked to four unsprung masses (axles of the vehicle), as shown in Fig. 1 and considering the definition of variables according to Tab. 2.

2.1. Dynamic equations

The dynamic equations of the model are, Ikenaga *et al.* (2000):

Vertical movement of the body:

$$\begin{aligned}
 M_s \ddot{z} = & -M_s g - (K_{sfl} + K_{sfr} + K_{srl} + K_{srr})z - (B_{sfl} + B_{sfr} + B_{srl} + B_{srr})\dot{z} + \\
 & + (aK_{sfl} + aK_{sfr} - bK_{srl} - bK_{srr})\theta + (aB_{sfl} + aB_{sfr} - bB_{srl} - bB_{srr})\dot{\theta} + K_{sfl}z_{ufl} + \\
 & + B_{sfl}\dot{z}_{ufl} + K_{sfr}z_{ufr} + B_{sfr}\dot{z}_{ufr} + K_{srl}z_{url} + B_{srl}\dot{z}_{url} + K_{srr}z_{urr} + B_{srr}\dot{z}_{urr}
 \end{aligned} \quad (1)$$

Pitch movement of the body:

$$\begin{aligned}
 I_{yy} \ddot{\theta} = & (aK_{sfl} + aK_{sfr} - bK_{srl} - bK_{srr})z + (aB_{sfl} + aB_{sfr} - bB_{srl} - bB_{srr})\dot{z} - \\
 & - (a^2 K_{sfl} + a^2 K_{sfr} + b^2 K_{srl} + b^2 K_{srr})\theta - (a^2 B_{sfl} + a^2 B_{sfr} + b^2 B_{srl} + b^2 B_{srr})\dot{\theta} - \\
 & - aK_{sfl}z_{ufl} - aB_{sfl}\dot{z}_{ufl} - aK_{sfr}z_{ufr} - aB_{sfr}\dot{z}_{ufr} + bK_{srl}z_{url} + bB_{srl}\dot{z}_{url} + bK_{srr}z_{urr} + bB_{srr}\dot{z}_{urr}
 \end{aligned} \quad (2)$$

Roll movement of the body:

$$\begin{aligned}
 I_{xx} \ddot{\varphi} = & -0,25w^2 (K_{sfl} + K_{sfr} + K_{srl} + K_{srr}) \varphi - \\
 & -0,25w^2 (B_{sfl} + B_{sfr} + B_{srl} + B_{srr}) \dot{\varphi} + 0,5wK_{sfl} z_{ufl} + 0,5wB_{sfl} \dot{z}_{ufl} - 0,5wK_{sfr} z_{ufr} - \\
 & -0,5wB_{sfr} \dot{z}_{ufr} + 0,5wK_{srl} z_{url} + 0,5wB_{srl} \dot{z}_{url} - 0,5wK_{srr} z_{urr} - 0,5wB_{srr} \dot{z}_{urr}
 \end{aligned} \tag{3}$$

Vertical movement of the left front axle:

$$\begin{aligned}
 M_{ufl} \ddot{z}_{ufl} = & -M_{ufl} g + K_{sfl} z + B_{sfl} \dot{z} - aK_{sfl} \theta - aB_{sfl} \dot{\theta} + 0,5wK_{sfl} \varphi + 0,5wB_{sfl} \dot{\varphi} - \\
 & - (K_{sfl} + K_{ufl}) z_{ufl} - B_{sfl} \dot{z}_{ufl} + K_{ufl} z_{rfl}
 \end{aligned} \tag{4}$$

Vertical movement of the right front axle:

$$\begin{aligned}
 M_{ufr} \ddot{z}_{ufr} = & -M_{ufr} g + K_{sfr} z + B_{sfr} \dot{z} - aK_{sfr} \theta - aB_{sfr} \dot{\theta} - 0,5wK_{sfr} \varphi - 0,5wB_{sfr} \dot{\varphi} - \\
 & - (K_{sfr} + K_{ufr}) z_{ufr} - B_{sfr} \dot{z}_{ufr} + K_{ufr} z_{rfr}
 \end{aligned} \tag{5}$$

Vertical movement of the left rear axle:

$$\begin{aligned}
 M_{url} \ddot{z}_{url} = & -M_{url} g + K_{srl} z + B_{srl} \dot{z} + bK_{srl} \theta + bB_{srl} \dot{\theta} + 0,5wK_{srl} \varphi + 0,5wB_{srl} \dot{\varphi} - \\
 & - (K_{srl} + K_{url}) z_{url} - B_{srl} \dot{z}_{url} + K_{url} z_{rrl}
 \end{aligned} \tag{6}$$

Vertical movement of the right rear axle:

$$\begin{aligned}
 M_{urr} \ddot{z}_{urr} = & -M_{urr} g + K_{srr} z + B_{srr} \dot{z} + bK_{srr} \theta + bB_{srr} \dot{\theta} - 0,5wK_{srr} \varphi - 0,5wB_{srr} \dot{\varphi} - \\
 & - (K_{srr} + K_{urr}) z_{urr} - B_{srr} \dot{z}_{urr} + K_{urr} z_{rrr}
 \end{aligned} \tag{7}$$

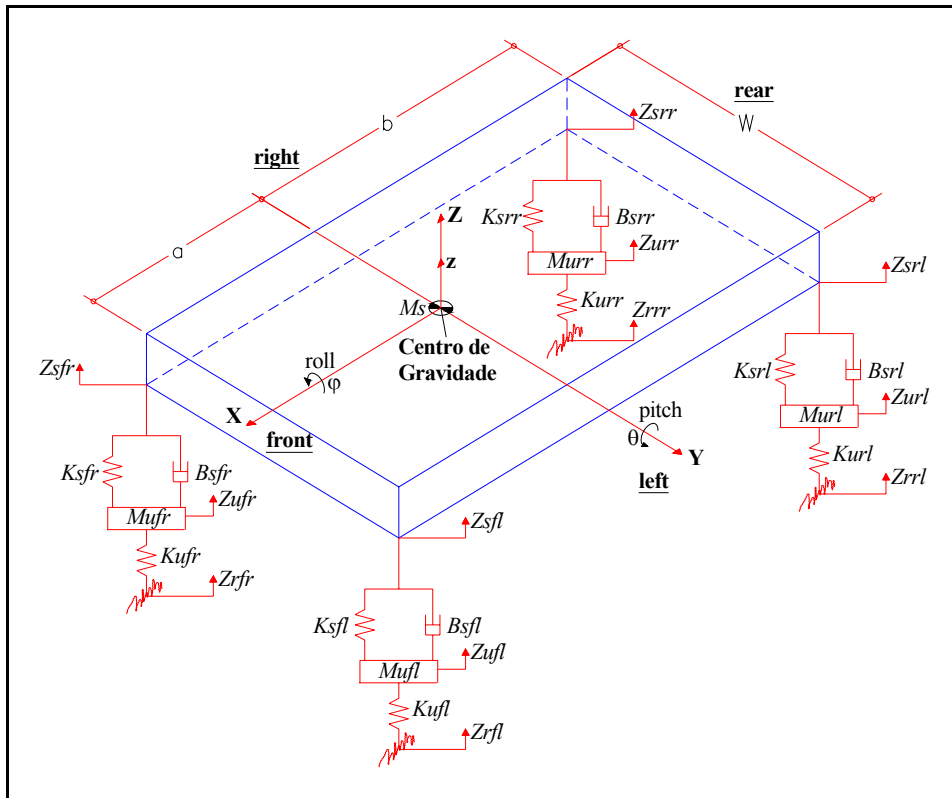


Figure 1. Vehicle model with seven degrees of freedom, Ikenaga *et al.* (2000).

2.2. Vehicle's excitement

For achievement of the road roughness profiles to be used in the dynamic analysis it is applied the Power Spectral Density (PSD) Function method, given by the Eq. (8) in $m^3/cycle$, according to Dodds and Robson (1973). This method uses experimental curves of spectral density for the characterization of typical road roughness profiles.

In this case, it was used the classification of roads and parameters as proposed by Dodds and Robson (1973). Seeing that the vehicle in analysis must support any class of road, it was adopted the profile of secondary roads in order to impose the most severe conditions. The characteristic values of the secondary roads used to determine the road profiles are shown in Tab. 1.

Table 1. Characteristic parameters of secondary roads.

Road class	Quality	$c \times 10^{-8} (m^3/cycle)$	w_1	w_2
Secondary roads	Medium	128		
	Low	512	2.28	1.428
	Very low	2048		

where the experimental roughness index c is associated to the road quality, n is the wave number, and w_1 and w_2 are mean values of the road quality. In this work, the PSD function is a simplified adaptation where w_1 and w_2 are assumed both equal to another variable w , taken as 2.5.

$$G_z(n) = c \cdot n^{-w} \tag{8}$$

One random road profile is applied to the left tires and another one to the right tires. Also, the front and the rear tire are exposed to the same road profile, but the function of the rear tire is delayed relative to the front signal. The vehicle moves with a velocity of 60 km/h and the power spectral density curve is composed by 12 components. The distance between the front tire and the rear one of the vehicle is equal to 2.5654 m. The road roughness profile or vertical excitation for each tire can be observed in Figs. 2 and 3.

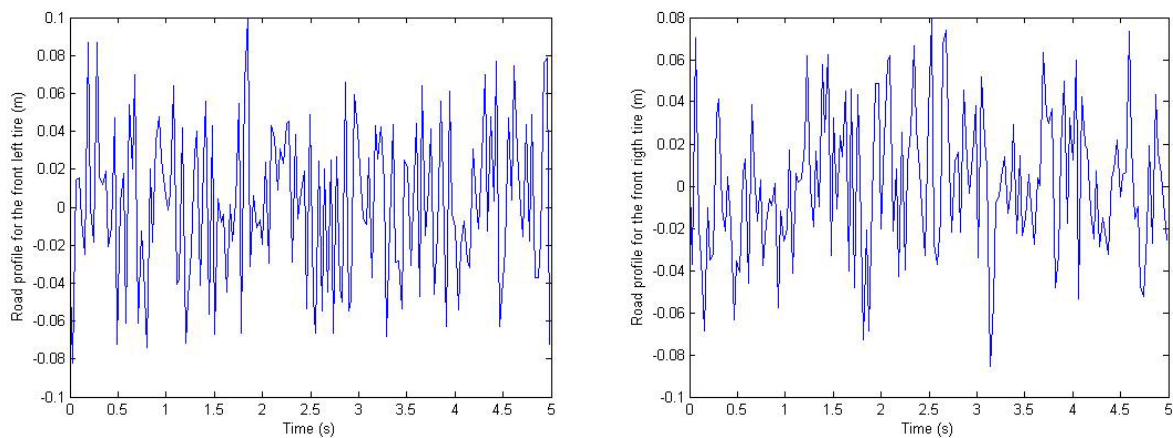


Figure 2. Roughness profile for a secondary road of very low quality acting at the front tires.

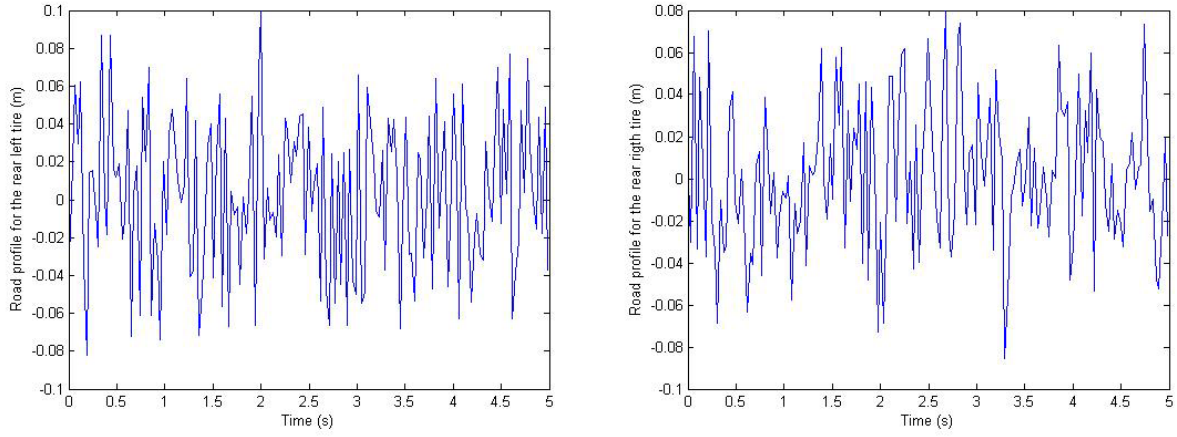


Figure 3. Roughness profile for a secondary road of very low quality acting at the rear tires.

3. PARAMETERS OPTIMIZATION OF THE PASSIVE SUSPENSION

In order to perform the optimization of the vertical dynamics of the vehicle, Rill (2004) proposes one merit function ϵ combining comfort and safety parts as expressed by the Eq. (9), where the gravitational acceleration g and the tire preload F_T^0 were used to weight the comfort and safety parts.

$$\text{Minimize } \epsilon_{G_c}^2 = \int_{t_i}^{t_n} \left\{ \left(\frac{\ddot{z}}{g} \right)^2 + \left(\frac{K_s z}{M_s g} \right)^2 + \left(\frac{K_u z_u}{F_T^0} \right)^2 \right\} dt \quad (9)$$

The first two terms of the Eq. (9) are associated with the comfort and the last one with the safety. Then, the adopted objective function ϵ to optimize is given by the Eq. (10).

$$\begin{aligned} \text{Minimize } \epsilon_{\{K_s, B_s\} \in \mathbb{R}^n}^2 &= \int_{t_i}^{t_n} \left\{ \left(\frac{\ddot{z}}{g} \right)^2 + \left(\frac{K_s z}{M_s g} \right)^2 + \left(\frac{K_u z_u}{F_T^0} \right)^2 \right\} dt \\ \text{subject to: } & (K_s)_{\min} < K_s < (K_s)_{\max} \\ & (B_s)_{\min} < B_s < (B_s)_{\max} \\ & (z_u)_{\min} < z_u < (z_u)_{\max} \end{aligned} \quad (10)$$

where,

- \ddot{z} : acceleration of the sprung mass, (m/s²),
- K_s : stiffness coefficient of the suspension, (N/m),
- z : vertical displacement of the sprung mass, (m),
- M_s : sprung mass, (kg),
- B_s : damping coefficient of the suspension, (N/(m/s)),
- z_u : vertical displacement of the unsprung mass, (m),
- M_u : unsprung mass, (kg);
- K_u : vertical tire stiffness, (N/m);
- F_T^0 : tire preload equal to $(M_s + M_u)g$, (kg);

In this work, the optimization variables are the stiffness and the damping coefficients of the suspension, starting with the initial values from He (2003) and considering the bounds given by the Tab. 2.

The minimization is realized through the *fmincon* Matlab® function, which attempts to find a constrained minimum of a scalar function of several variables starting at an initial estimate. The problem is referred to as constrained nonlinear optimization or nonlinear programming.

4. RESULTS' ANALYSIS

For the objective function given by the Eq. (10), the Tab. 3 shows the coefficients of stiffness and damping for the suspension before and after the optimization. It is observed that the optimized values of the damping coefficients are

close to the lower bounds of the variables, indicating that the function is directly proportional to these coefficients. The initial value of the objective function is 56.37 and after the optimization is equal to 55.84.

Table 2. Vehicle parameters.

Variable	Description	Unit	Value	Bounds
K_{sfl}	Stiffness of the left front suspension	N/m	9980	8000 – 12000
K_{sfr}	Stiffness of the right front stiffness	N/m	9980	8000 – 12000
K_{srl}	Stiffness of the left rear suspension	N/m	11295	8000 – 12000
K_{srr}	Stiffness of the right rear suspension	N/m	11295	8000 – 12000
B_{sfl}	Damping of the left front suspension	N/(m/s)	1007	800 – 1200
B_{sfr}	Damping of the right front suspension	N/(m/s)	1007	800 – 1200
B_{srl}	Damping of the left rear suspension	N/(m/s)	1041	800 – 1200
B_{srr}	Damping of the right rear suspension	N/(m/s)	1041	800 – 1200
K_u	Front or rear tire stiffness	N/m	77950	-
M_s	Sprung or body mass	kg	501.1	-
M_{ufl}	Left front unsprung mass	kg	14.25	-
M_{ufr}	Right front unsprung mass	kg	14.25	-
M_{url}	Left rear unsprung mass	kg	27.35	-
M_{urr}	Right rear unsprung mass	kg	27.35	-
z_u	Vertical displacement of the unsprung mass	m	-	0.127 – 2.54e-6

Table 3. Suspension coefficients.

Coefficient	Description	Initial value	Optimized value
B_{sfl} , B_{sfr}	Damping of the front suspension	1007 N/(m/s)	800 N/(m/s)
B_{srl} , B_{srr}	Damping of the rear suspension	1041 N/(m/s)	800 N/(m/s)
K_{sfl} , K_{sfr}	Stiffness of the front suspension	9980 N/m	9885 N/m
K_{srl} , K_{srr}	Stiffness of the rear suspension	11295 N/m	11200 N/m

Some comparative results are shown in Figs. 4 to 6.

Figure 4 shows the comparative in body acceleration before and after the optimization. Although the curves of acceleration seem similar, the RMS value before optimization is equal to 6.71 and after optimization is equal to 6.36, indicating 5.2% of reduction in 3 seconds of simulation.

Figure 5 shows the comparative in body velocity before and after the optimization. Although for the first second of simulation the module of the optimized velocity grows due to the equilibrium stabilization, its posterior behavior shows a reduction in oscillation if compared with the non-optimized value.

Figure 6 shows the comparative in body displacement before and after the optimization. Although the optimized value initially shows the displacement larger than the non-optimized case because of the less rigid suspension, its posterior behavior shows a reduction in the amplitude of oscillation if compared with the non optimized value.

Finally, it is observed that this work looks for the same set of coefficients for the front suspension and another for the rear one, with the practical purpose of disposing with two types of suspensions.

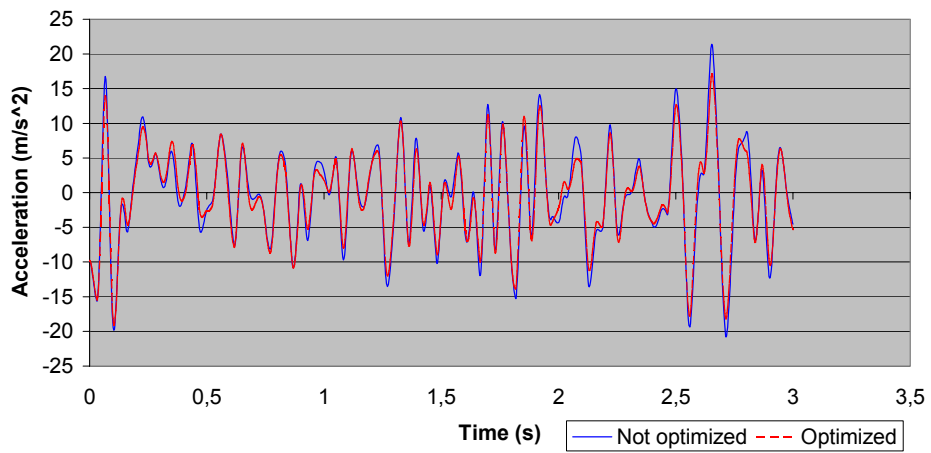


Figure 4. Comparative of body acceleration.

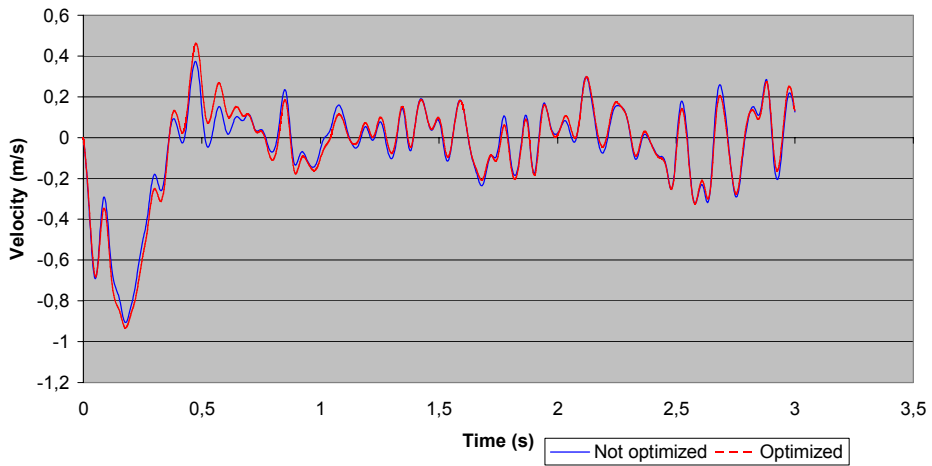


Figure 5. Comparative of body velocity.

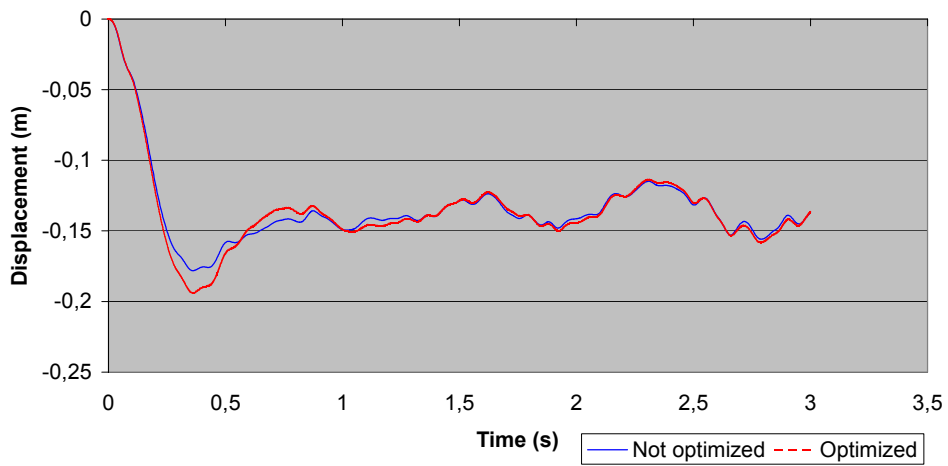


Figure 6. Comparative of body displacement.

5. CONCLUSIONS

The vehicle comfort associated with the vertical dynamics is optimized modifying the coefficients of stiffness and damping of the suspensions. It is observed that the optimized values of the damping coefficients are close to the lower bounds of the variables, indicating that the objective function is proportional to these coefficients. Incorporating one restriction associated with the suspension spring travel must modify this condition.

Although the curves of body accelerations seem similar, the RMS value before optimization is equal to 6.71 and after optimization is equal to 6.24, indicating 7% of reduction during 3 seconds of simulation.

The comparative in body velocity before and after the optimization shows that for the first second of simulation the absolute value of the optimized velocity grows because of the equilibrium stabilization, but its posterior behavior shows a reduction in the oscillation if compared with the non optimized value.

The comparative in body displacement before and after the optimization shows that for the first second of simulation the optimized value is larger than the non optimized case because of the less rigid suspension. Also, its posterior behavior shows a reduction in the amplitude of the oscillation if compared with the non optimized value.

6. ACKNOWLEDGEMENTS

The accomplishment of this work counted with one scientific research scholarship, PIBIC CNPq-UFRGS (M.M) and BIC/FAPERGS (V.L.B.N.).

7. REFERENCES

- Dodds, C.J. and Robson, J.D., 1973, "The Description of Road Surface Roughness", *Journal of Sound and Vibration*, Vol. 31, pp. 175-183.
- He, Y., 2003, "Design of Rail Vehicles with Passive and Active Suspensions Using Multidisciplinary Optimization, Multibody Dynamics, and Genetic Algorithms", Ph.D. Thesis in Mechanical Engineering, University of Waterloo, Ontario, Canada.
- Ikenaga, S., Lewis, F.L., Campos, J. and Davis, L., 2000, "Active Suspension Control of Ground Vehicle Based on a Full-Vehicle Model", *Proceedings of the American Control Conference*, Chicago, Illinois, pp. 4019-4024.
- Motta, D.D.S. and Zampieri, D.E., 2005, "Modeling of a Vehicle Suspension with Non Linear Elements and Performance Comparison to a Semi-Active Model", *Proceedings of the 18th International Congress of Mechanical Engineering*, Ouro Preto, MG, Brazil.
- Rill, G., 2004, "Vehicle Dynamics. Lecture Notes", Fachhochschule Regensburg University of Applied Sciences.

8. RESPONSIBILITY NOTICE

The authors are the only responsible for the printed material included in this paper.